Journal of Multidisciplinary Engineering Science and Technology (JMEST)
ISSN: 2458-9403
Vol. 6 Issue 11, November - 2019

Viscoelastic-plastic Materials: Parameter Estimate and Numerical Simulation of Experimental Tests

Bruno Crisman
Department of Engineering and Architecture
University of Trieste, P.le Europa 1
34127 Trieste, Italy

Alfonso Nappi
Department of Engineering and Architecture
University of Trieste, P.le Europa 1
34127 Trieste, Italy

***Abstract*—This paper is focused on a *generalized Voigt model* applicable to three-dimensional stress states and suitable for the numerical analysis of structural systems made of bituminous mixtures. In this context, it is noted that *viscoelastic-plastic models*, in principle, can be easily and effectively utilized in the field of pavement analysis and design, since they require limited computational effort. In fact, modern computers and well tested algorithms are definitely adequate for the nonlinear analysis of structural systems, although elastic discrete models are obviously easier to handle, because the response to external actions is obtained by solving a single linear system of equations. Instead, even in the case of quasi-static loading conditions, viscous materials require an incremental analysis, which is carried out by subdividing the load history into a finite number of time-steps. In addition, when plastic deformations are considered, an iterative algorithm is needed to find the non-reversible strains during each step.**

The main objective of the paper is the estimate of the mechanical properties, since any material model can be used if it is possible to determine its parameters, preferably by means of simple testing procedures. Therefore, a linear elastic analysis (when reasonably applicable) represents the most appealing option, thanks to the additional advantage provided by the easy estimate of elastic properties, while the parameters that govern the response of viscous materials inevitably imply more difficult challenges—and further efforts are required in the presence of plastic strains.

However, it is shown that the parameters concerned with viscoelastic-plastic materials can actually be estimated on the basis of traditional, simple compression tests on cylindrical specimens. Optimal values can be found by using classical system identification procedures, but we preferred to give attention to some special features of the material model discussed here and eventually implemented a *trial and error algorithm* specifically designed for viscoelastic-plastic specimens. Numerical simulations do suggest that the proposed approach is suitable and effective for the estimate of the parameters, which are needed to characterize these materials.

Keywords—bituminous mixtures; deviatoric and isotropic stress/strain components; discrete numerical models; finite element method; parameter estimate; structural analysis; system identification; viscoelastic-plastic materials; Voigt model

I. INTRODUCTION

The *bituminous mixtures* which are commonly used as flexible pavement materials are generally characterized by focusing on a significant stiffness parameter. In this context, a special role is often played by the *complex modulus* or the *resilient modulus*, which essentially quantify an average/equivalent elastic stiffness. These parameters can be determined by studying the response of convenient test specimens subjected to repeated cyclic stresses.

Of course, if the elastic stiffness (or a sort of equivalent elastic stiffness) is the only mechanical property of interest, the end result is that the structural behavior of pavements is described through a simple elastic analysis [1-3] and a *viscoelastic problem* is changed into an associated elastic problem.

Nonetheless, a little more effort (with minor impact in view of today's computational tools) is required, if the behavior of *bituminous mixtures* is described by considering *viscoelastic-plastic material models*, which can take into account the non-reversible strains and the consequential permanent deformation of pavements (*rutting*) caused by repeated loads.

Actually, *viscoelastic-plastic materials* can be efficiently applied in the framework of finite element discrete models and are able to simulate the response to a wide range of load conditions. For instance, these include quasi-static loads, load pulses (with convenient rest periods) and sinusoidal external forces, as shown in Fig. 1. Here, the plots are concerned with a cylindrical test specimen, which was modelled by exploiting the presence of two planes of symmetry and considering a convenient portion (Fig. 2a). The mesh is characterized by a regular pattern (Fig. 2b), for which it is possible to recognize a certain number of layers and dihedral angles. Of course, the number of

elements belonging to a given layer and a given dihedral angle is always the same: for instance, there are three elements that satisfy this condition in the case of the discrete model in Fig. 2b, which features four layers and four dihedral angles. In the end, the total number of elements concerned with the mesh of Fig. 2b is 48 (=4x4x3) and the total number of nodes is 279 (since 15-node pentahedral and 20-node hexahedral elements have been used).

Coming back to the plots in Fig. 1, it should just be noted that the curve on the left refers to a quasi-static uniaxial compression load applied during 1 s, maintained constant for 19 s and removed during 1 s; the curve in the middle is concerned with an indirect tension test simulated by considering pulse loads characterized by haversine waveforms, a rise time of 0.125 s and a repetition period of 3 s; the curve on the right shows the response to a sinusoidal compressive load (with a 2 Hz frequency) ranging between zero and the peak value.

In view of these graphs and of the typical behavior of bituminous mixtures, *viscoelastic-plastic materials* appear to be suitable for the structural analysis of pavements, but the relevant parameters are needed in order to obtain reliable results.

Thus, the aim of the present paper is the estimate of the parameters, which are required to define the mechanical properties of macroscopically homogeneous *viscoelastic-plastic materials* subjected to multiaxial stress states.

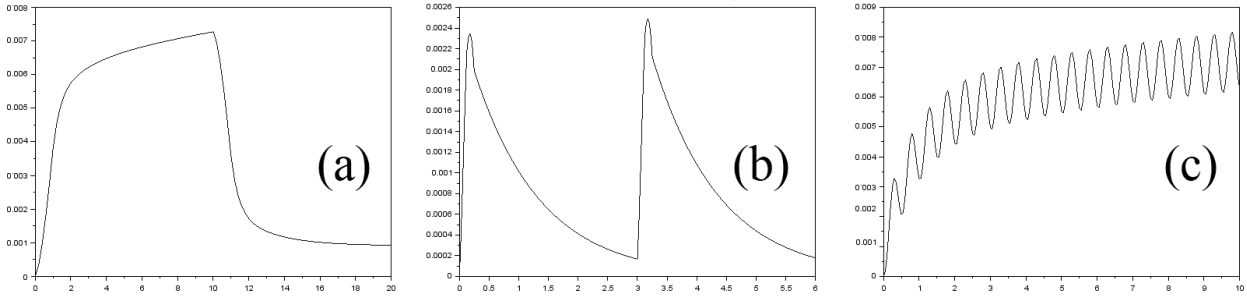

Fig. 1. *Typical displacement-time plots due to different load conditions (units: mm, s).*

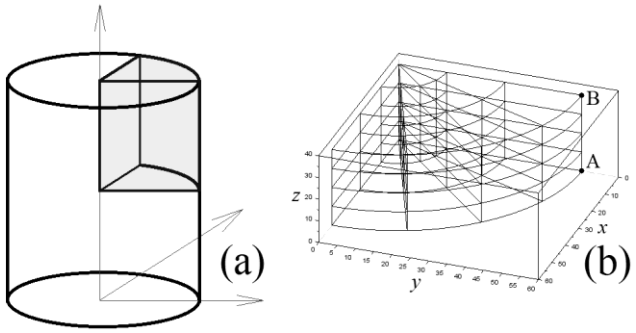

Fig. 2. *Test specimen and discrete model.*

Namely, we will discuss a generalization of the classical *Voigt model* (concerned with uniaxial stresses) by considering three-dimensional stress states. We will also show that the relevant mechanical properties can be determined by exploiting classical compression tests on cylindrical specimens subjected to uniaxial quasi-static loads. Incidentally, it will also be observed that the estimates only depend on the actual material, while the test specimen does not have any influence on the results.

It is worth noting that this final remark is not so obvious and insignificant as it might seem at first glance. For instance, as reported in the specialized literature and in documents concerned with standard testing procedures [4], the *indirect tension test* can be used to estimate a *stiffness modulus*, but the final outcome does not appear to be *test-independent*.

As well known, the *indirect tension test* requires a cylindrical specimen, which is subjected to compression loads along two opposite surface segments (s_1, s_2) parallel to the cylinder axis (for instance, s_1 can be the segment AB in Fig. 2b). Then, if we measure the diametral deformation of the specimen δ (in the direction which is orthogonal to the plane passing through the segments s_1 and s_2), we obtain an estimate of the *stiffness modulus* S_M by setting $S_M=F.(\nu+0.27)/(\delta.w)$, where F is the applied load, ν Poisson's ratio and w the thickness of the specimen [4].

In order to use a formula of this kind and obtain unique results, a well-defined size of the specimen should be specified. Instead, different diameters are usually recommended (*e.g.*, ranging between 80 and 200 mm [4]), as well as different values of the thickness (*e.g.*, ranging between 30 and 75 mm [4]).

The inevitable consequence is that the estimate of the *stiffness modulus* is *test-dependent* or, if you prefer, *specimen-dependent*, because the *diametral deformation* δ does depend on the specimen diameter, unless the *thickness* of the cylinder tends to infinite. This fact can be easily checked through a simple finite element elastic analysis whose results are summarized in Table I.

TABLE I. INFLUENCE OF THE SPECIMEN THICKNESS AND DIAMETER ON THE DIAMETRAL DEFORMATION.

d [mm]	w [mm]	F [N]	F/w	δ [mm]
80	30	112.50	3.75	0.0022896
80	50	187.50	3.75	0.0021767
80	60	225.00	3.75	0.0021014
80	75	281.25	3.75	0.0020083
80	800	3000.00	3.75	0.0020827
200	30	112.50	3.75	0.0023245
200	50	187.50	3.75	0.0023136
200	60	225.00	3.75	0.0023049
200	75	281.25	3.75	0.0022880
200	2000	7500.00	3.75	0.0020815

We assumed a linear elastic homogeneous material and different diameters d (80 mm, 200 mm), combined with different values of the specimen thickness w (30 mm, 50 mm, 75 mm, 10d, where the product 10d is meant to approximate the case of a cylinder characterized by an infinite length).

The displacements in Tab. 1 were obtained by setting Young's modulus equal to 2000 MPa and Poisson's ratio equal to 0.35. The load per unit length (F/w) was maintained constant and the diameter did not appear to have any significant influence on δ only when w= 10d.

II. VISCOELASTIC-PLASTIC MATERIALS AND 3D FINITE ELEMENT ANALYSIS

In this Section, we will briefly discuss a *generalized Voigt model* and its possible applications to three-dimensional discrete models suitable for a finite element structural analysis. Note that, in this context, the term *generalized* is referred to the possible presence of non-reversible strains and to the fact that multiaxial stress states can be dealt with.

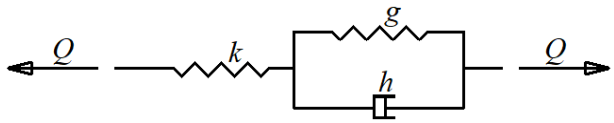

Fig. 3. *Mechanical model for viscoelastic systems.*

A convenient starting point is the classical mechanical model in Fig. 3, concerned with *viscoelastic materials* [5] and uniaxial stress states. Here, we have a linear elastic spring, characterized by the stiffness parameter k, combined with a second elastic spring (whose stiffness parameter is g) and a *viscous element*, whose response (in turn) is governed by the coefficient h. Such viscous element, in parallel with the second spring, is typical of Voigt's model. The relevant governing equation reads

$$Q = k\,u = g\,u_V + h\,\dot{u}_V \tag{1}$$

where u represents the elongation of the first spring and u_V is the viscous component of the total displacement (which corresponds to the elongation of the second spring), while the last term in (1) denotes the time derivative of u_V.

If we consider elastic moduli and a convenient parameter η instead of h, the above equation can be rewritten in terms of stresses σ and strains ε or ξ (*elastic* and *viscous* components of the strains):

$$\sigma = E\,\varepsilon = E^*\,\xi + \eta\,\dot{\xi} \tag{2}$$

Next, it is possible to derive a more general equation by introducing a relationship that takes into account multiaxial stress states. This can be done by considering two separate contributions, related to *isotropic* and *deviatoric* stresses/strains:

$$\sigma_m = K\,\varepsilon^v = K^*\,\xi^v + \eta_V\,\dot{\xi}^v \tag{3a}$$

$$s_{ij} = 2\,G\,e_{ij} = 2\,G^*\,d_{ij} + 2\,\eta_D\,\dot{d}_{ij} \tag{3b}$$

Here, $\sigma_m=(\sigma_{11}+\sigma_{22}+\sigma_{33})/3$ is the mean stress, $\varepsilon^v=\varepsilon_{11}+\varepsilon_{22}+\varepsilon_{33}$ the volumetric elastic strain, ξ^v the corresponding viscous volumetric strain, s_{ij} a deviatoric stress component and d_{ij} a viscous deviatoric strain component, while K and K^* denote bulk moduli, G and G^* shear moduli, η_V and η_D coefficients of viscosity.

Equations (3) can be combined and rewritten in matrix form in order to obtain relationships, which will be easier to handle, when we introduce discrete finite element models:

$$\boldsymbol{\sigma} = \boldsymbol{\sigma}_m + \mathbf{s} = 3\,K\,\boldsymbol{\varepsilon}_m + 2\,G\,\mathbf{e} = \\ = 3\,K^*\,\boldsymbol{\xi}_m + 2\,G^*\,\mathbf{d} + 3\,\eta_V\,\dot{\boldsymbol{\xi}}_m + 2\,\eta_D\,\dot{\mathbf{d}} \tag{4}$$

where $\boldsymbol{\sigma}=[\sigma_{11}\ \sigma_{22}\ \sigma_{33}\ \sigma_{12}\ \sigma_{23}\ \sigma_{31}]^T$, $\boldsymbol{\sigma}_m=[\sigma_m\ \sigma_m\ \sigma_m\ 0\ 0\ 0]^T$, $\mathbf{s}=[s_{11}\ s_{22}\ s_{33}\ s_{12}\ s_{23}\ s_{31}]^T$. Similarly, $\boldsymbol{\varepsilon}_m=[\varepsilon^v/3\ \varepsilon^v/3\ \varepsilon^v/3\ 0\ 0\ 0]^T$, $\mathbf{e}=[e_{11}\ e_{22}\ e_{33}\ e_{12}\ e_{23}\ e_{31}]^T$. Of course, the vectors $\boldsymbol{\xi}_m$ and $\mathbf{d}$ are fully analogous to $\boldsymbol{\varepsilon}_m$ and $\mathbf{e}$ (with the significant entries ξ^v and d_{ij} instead of ε^v and e_{ij}).

Note that an increment of the strain energy per unit volume is given by the expression ($\boldsymbol{\sigma}_m^T\,\mathrm{d}\boldsymbol{\varepsilon}_m+\mathbf{s}^T\,\mathbf{M}\,\mathrm{d}\mathbf{e}$) or, alternatively, ($3K\,\boldsymbol{\varepsilon}_m^T\,\mathrm{d}\boldsymbol{\varepsilon}_m+2G\,\mathbf{e}^T\,\mathbf{M}\,\mathrm{d}\mathbf{e}$), where $\mathbf{M}$ is a diagonal matrix whose significant entries are $M_{11}=M_{22}=M_{33}=1$ and $M_{44}=M_{55}=M_{66}=2$. In fact, the scalar products ($\boldsymbol{\sigma}_m^T\,\mathrm{d}\boldsymbol{\varepsilon}_m$) and ($3K\,\boldsymbol{\varepsilon}_m^T\,\mathrm{d}\boldsymbol{\varepsilon}_m$) correspond to $\sigma_m\,\mathrm{d}\varepsilon^v$, while the scalar products ($\mathbf{s}^T\,\mathbf{M}\,\mathrm{d}\mathbf{e}$) and ($2G\,\mathbf{e}^T\,\mathbf{M}\,\mathrm{d}\mathbf{e}$) correspond to $s_{ij}\,\mathrm{d}e_{ij}$ (with i and j ranging between 1 and 3).

Now, it is possible to derive the elastic stiffness matrix of any finite element by applying the principle of virtual displacements, which requires the computation of some integrals concerned with the volume and the boundary (or external surface) of each element:

$$\begin{aligned}&\int\{\boldsymbol{\sigma}_m+\mathbf{s}\}^{\mathrm{T}}\{\delta\boldsymbol{\varepsilon}_m+\mathbf{M}\,\delta\mathbf{e}\}\,dV=\\&=\int\{3K\,\boldsymbol{\varepsilon}_m+2G\,\mathbf{e}\}^{\mathrm{T}}\{\delta\boldsymbol{\varepsilon}_m+\mathbf{M}\,\delta\mathbf{e}\}\,dV=\\&=\int\mathbf{b}^{\mathrm{T}}\,\delta\mathbf{u}\,dV+\int\mathbf{f}^{\mathrm{T}}\,\delta\mathbf{u}\,dS\end{aligned}\tag{5}$$

Here, the vectors $\mathbf{u}$, $\mathbf{b}$ and $\mathbf{f}$ refer to elastic displacements, body forces and surface forces, usually defined with reference to local coordinates. As typical of finite element formulations, we can introduce a matrix of shape functions $\boldsymbol{\Phi}$, such that $\mathbf{u}=\boldsymbol{\Phi}\,\mathbf{u}_N$, as well as the matrices $\mathbf{B}_V$ and $\mathbf{B}_D$ of convenient derivatives of the entries of the matrix $\boldsymbol{\Phi}$, in order to set $\boldsymbol{\varepsilon}_m=\mathbf{B}_V\,\mathbf{u}_N$ and $\mathbf{e}=\mathbf{B}_D\,\mathbf{u}_N$, if $\mathbf{u}_N$ denotes the vector of the nodal elastic displacements of the element. Hence, we obtain

$$\begin{aligned}&\int\{\boldsymbol{\sigma}_m+\mathbf{s}\}^{\mathrm{T}}\{\delta\boldsymbol{\varepsilon}_m+\mathbf{M}\,\delta\mathbf{e}\}\,dV=\\&=\delta\mathbf{u}_N^{\mathrm{T}}\left[\int 3K\,\mathbf{B}_V^{\mathrm{T}}\,\mathbf{B}_V\,dV\right]\mathbf{u}_N+\\&+\delta\mathbf{u}_N^{\mathrm{T}}\left[\int 2G\,\mathbf{B}_D^{\mathrm{T}}\,\mathbf{M}\,\mathbf{B}_D\,dV\right]\mathbf{u}_N\end{aligned}\tag{6}$$

and

$$\begin{aligned}&\int\mathbf{b}^{\mathrm{T}}\,\delta\mathbf{u}\,dV+\int\mathbf{f}^{\mathrm{T}}\,\delta\mathbf{u}\,dS=\\&=\delta\mathbf{u}_N^{\mathrm{T}}\left\{\int\boldsymbol{\Phi}^{\mathrm{T}}\,\mathbf{b}\,dV+\int\boldsymbol{\Phi}^{\mathrm{T}}\,\mathbf{f}\,dS\right\}=\delta\mathbf{u}_N^{\mathrm{T}}\,\mathbf{q}_N\end{aligned}\tag{7}$$

where $\mathbf{q}_N$ represents the traditional vector of equivalent nodal loads.

As suggested by (6), the scalar products between vectors concerned with isotropic and deviatoric quantities disappear, since $\boldsymbol{\varepsilon}_m=[\varepsilon^v/3\;\;\varepsilon^v/3\;\;\varepsilon^v/3\;\;0\;\;0\;\;0]^{\mathrm{T}}$, while the first three entries of the vector $\{\mathbf{M}\,\delta\mathbf{e}\}$ are δe_{11}, δe_{22}, δe_{33}. Hence, in full agreement with well-known properties related to isotropic and deviatoric quantities, the product $(\boldsymbol{\sigma}_m^{\mathrm{T}}\,\mathbf{M}\,\delta\mathbf{e})$ is zero, since $\boldsymbol{\sigma}_m=3K\boldsymbol{\varepsilon}_m$ and $\varepsilon^v=e_{11}+e_{22}+e_{33}$. For similar reasons, we get $\mathbf{s}^{\mathrm{T}}\,\delta\boldsymbol{\varepsilon}_m=0$.

After computing the integrals in the square brackets of (6), we determine the entries of the stiffness matrices related to the bulk modulus K (say $\mathbf{K}'$) and the shear modulus G (say $\mathbf{K}''$). Of course, we can set $[\mathbf{K}'+\mathbf{K}'']=\mathbf{K}_e$, if $\mathbf{K}_e$ represents the traditional elastic stiffness matrix of the generic *e-th* element. Therefore, we can write the equation

$$\delta\mathbf{u}_N^{\mathrm{T}}\,[\mathbf{K}'+\mathbf{K}'']\,\mathbf{u}_N=\delta\mathbf{u}_N^{\mathrm{T}}\,\mathbf{K}_e\,\mathbf{u}_N\tag{8}$$

Obviously, (7) must be equal to (8) for any $\delta\mathbf{u}_N$. This property implies the equilibrium equation $\mathbf{K}_e\,\mathbf{u}_N=\mathbf{q}_N$, from which we can proceed with the assembly process (in order to include the contributions due to all elements) and obtain the system of equations $\mathbf{K}\,\mathbf{U}=\mathbf{Q}$, where $\mathbf{Q}$ and $\mathbf{U}$ are obviously referred to a global system of coordinates. Alternatively, we can end up with the fully analogous linear system $[\mathbf{K}_V+\mathbf{K}_D]\,\mathbf{U}=\mathbf{Q}$ (with $\mathbf{K}=\mathbf{K}_V+\mathbf{K}_D$) and continue to distinguish the contributions due to the stiffness parameters K and G.

Next, we should apply the principle of virtual work by considering the same external forces and the quantities concerned with *viscous strains*. Thus, for any finite element we obtain

$$\begin{aligned}&\int\{3\,K^*\,\boldsymbol{\xi}_m+2\,G^*\,\mathbf{d}+3\,\eta_V\,\boldsymbol{\xi}_m+2\,\eta_D\,\mathbf{d}\}^{\mathrm{T}}\{\delta\boldsymbol{\xi}_m+\mathbf{M}\,\delta\mathbf{d}\}\,dV=\\&=\delta\hat{\mathbf{u}}_N^{\mathrm{T}}\,\mathbf{q}_N\end{aligned}\tag{9}$$

Here, we can deal with the term on the left hand side exactly as we did with the second term in the chain of equations (5), by setting $\boldsymbol{\xi}_m=\mathbf{B}_V\,\hat{\mathbf{u}}_N$ and $\mathbf{d}=\mathbf{B}_D\,\hat{\mathbf{u}}_N$, where $\hat{\mathbf{u}}_N$ denotes nodal viscous displacements, usually referred to a local coordinate system. Finally, the linear system $[\mathbf{S}_V+\mathbf{S}_D]\,\dot{\hat{\mathbf{U}}}+[\mathbf{H}_V+\mathbf{H}_D]\,\hat{\mathbf{U}}=\mathbf{Q}$ will be derived by means of obvious substitutions. In this relationship $\hat{\mathbf{U}}$ collects all the nodal viscous displacements referred to global coordinates, $\mathbf{S}_V$ and $\mathbf{S}_D$ are the contributions to the elastic stiffness matrix concerned with the time-dependent response (*i.e.*, the contributions due to the stiffness parameters K^* and G^*), $\mathbf{H}_V$ and $\mathbf{H}_D$ are the matrices that govern the response to the time derivatives of $\hat{\mathbf{U}}$ (or, in other words, are the matrices that depend on the viscous parameters η_V and η_D).

At this stage, it is possible to carry out an incremental *viscoelastic analysis* by subdividing the load history into a given number of time-steps. As typical of time-dependent problems, we can assume that we know the configuration of the system (in terms of displacements $\mathbf{U}=\mathbf{U}_o$ and $\hat{\mathbf{U}}=\hat{\mathbf{U}}_o$) at the beginning of each step, say at time $t=t_o$, when the vector of the equivalent nodal loads is $\mathbf{Q}=\mathbf{Q}_o$. Of course, at time $t=0$, we have $\mathbf{U}_o=\mathbf{0}$, $\hat{\mathbf{U}}_o=\mathbf{0}$, $\mathbf{Q}_o=\mathbf{0}$.

Thus, we can compute the vector $\Delta\mathbf{U}$, which solves the elastic problem $\mathbf{K}\,\Delta\mathbf{U}=\Delta\mathbf{Q}$, where $\Delta\mathbf{Q}$ is the load increment concerned with the present time step. Next, we need to satisfy the equation

$$\begin{aligned}&[\mathbf{S}_V+\mathbf{S}_D]\,\{\hat{\mathbf{U}}_o+\Delta\dot{\hat{\mathbf{U}}}\,(t-t_o)/\Delta t\}+[\mathbf{H}_V+\mathbf{H}_D]\,\dot{\hat{\mathbf{U}}}(t)=\\&=\mathbf{K}\,\{\mathbf{U}_o+\Delta\mathbf{U}\,(t-t_o)/\Delta t\}\end{aligned}\tag{10}$$

with $t_o\le t\le t_o+\Delta t$.

As we write the above equation, we implicitly assume a constant velocity $\Delta\dot{\hat{\mathbf{U}}}/\Delta t$ during the current time-step. The obvious consequence is a linear increment of the displacement $\Delta\hat{\mathbf{U}}$, while the vector $\{[\mathbf{H}_V+\mathbf{H}_D]\,\Delta\hat{\mathbf{U}}/\Delta t\}$ remains constant during the entire time-step. Therefore, the best compromise is to satisfy (10) at time $t=t_o+\Delta t/2$, when the terms which depend on $\Delta\mathbf{U}$ and $\Delta\dot{\hat{\mathbf{U}}}$ attain their mean values during the time interval between t_o and $t_o+\Delta t$. This implies the solution of the linear system

$$\begin{aligned}&[\mathbf{S}_V+\mathbf{S}_D]\,\{\hat{\mathbf{U}}_o+\tfrac{1}{2}\Delta\dot{\hat{\mathbf{U}}}\}+[\mathbf{H}_V+\mathbf{H}_D]\,\Delta\dot{\hat{\mathbf{U}}}/\Delta t=\\&=\mathbf{K}\,\{\mathbf{U}_o+\tfrac{1}{2}\Delta\mathbf{U}\}\end{aligned}\tag{11}$$

in which the only unknown is the vector $\Delta\dot{\hat{\mathbf{U}}}$.

When plastic strains are considered, we simply need to set $\boldsymbol{\sigma}_m=3K(\boldsymbol{\varepsilon}_m-\boldsymbol{\varepsilon}^{\mathrm{p}})$ and $\mathbf{s}=2G(\mathbf{e}-\mathbf{e}^{\mathrm{p}})$ instead of $\boldsymbol{\sigma}_m=3K\boldsymbol{\varepsilon}_m$ and $\mathbf{s}=2G\mathbf{e}$ in (4), since the elastic, reversible

components of the strains become ($\boldsymbol{\varepsilon}_m$-$\boldsymbol{\varepsilon}^p$) and ($\mathbf{e}$-$\mathbf{e}^p$), which must replace the vectors $\boldsymbol{\varepsilon}_m$ and $\mathbf{e}$ used in (4).

Then, by considering nodal displacements $\mathbf{u}_N$ which also include the plastic components, we easily derive a couple of integrals to be algebraically added to (6):

$$-\delta\mathbf{u}_N^{\mathrm{T}}\left\{\int 3K\,\mathbf{B}_V^{\mathrm{T}}\,\boldsymbol{\varepsilon}^p\,dV\right\}\mathbf{u}_N = -\delta\mathbf{u}_N^{\mathrm{T}}\left[\int 3K\,\mathbf{B}_V^{\mathrm{T}}\,\boldsymbol{\Phi}_\lambda\,dV\right]\boldsymbol{\lambda}_e = = -\delta\mathbf{u}_N^{\mathrm{T}}\,\mathbf{L}'\,\boldsymbol{\lambda}_e \quad (12a)$$

$$-\delta\mathbf{u}_N^{\mathrm{T}}\left\{\int 2G\,\mathbf{B}_D^{\mathrm{T}}\,\mathbf{M}\,\mathbf{e}^p\,dV\right\}\mathbf{u}_N = -\delta\mathbf{u}_N^{\mathrm{T}}\left[\int 2G\,\mathbf{B}_D^{\mathrm{T}}\,\mathbf{M}\,\boldsymbol{\Phi}_\mu\,dV\right]\boldsymbol{\mu}_e = -\delta\mathbf{u}_N^{\mathrm{T}}\,\mathbf{L}''\,\boldsymbol{\mu}_e \quad (12b)$$

where $\boldsymbol{\lambda}_e$ and $\boldsymbol{\mu}_e$ collect (for each element) the values of $\boldsymbol{\varepsilon}^p$ and $\mathbf{e}^p$ at convenient (internal) *strain points*, which usually coincide with points where the value of an integrand function is to be computed when numerical integration formulas are used. Therefore, $\boldsymbol{\Phi}_\lambda$=$\boldsymbol{\Phi}_\mu$ are the usual matrices of shape functions, which give the plastic strain components anywhere inside the elements, when $\boldsymbol{\varepsilon}^p$ and $\mathbf{e}^p$ (*i.e.*, vectors $\boldsymbol{\lambda}_e$ and $\boldsymbol{\mu}_e$) are known at the selected *strain points*.

In the end, instead of the system $\mathbf{K}\,\mathbf{U}$=$\mathbf{Q}$, we shall deal with the governing equation

$$\mathbf{K}\,\mathbf{U} - \mathbf{L}_V\,\boldsymbol{\lambda} - \mathbf{L}_D\,\boldsymbol{\mu} = [\mathbf{K}_V+\mathbf{K}_D]\,\mathbf{U} - \mathbf{L}_V\,\boldsymbol{\lambda} - \mathbf{L}_D\,\boldsymbol{\mu} = \mathbf{Q} \quad (13)$$

where $\boldsymbol{\lambda}$ and $\boldsymbol{\mu}$ collect the subvectors $\boldsymbol{\lambda}_e$ and $\boldsymbol{\mu}_e$. The same equation can also be written in incremental form:

$$\mathbf{K}\,\Delta\mathbf{U} - \mathbf{L}_V\,\Delta\boldsymbol{\lambda} - \mathbf{L}_D\,\Delta\boldsymbol{\mu} = [\mathbf{K}_V+\mathbf{K}_D]\,\Delta\mathbf{U} - \mathbf{L}_V\,\Delta\boldsymbol{\lambda} - \mathbf{L}_D\,\Delta\boldsymbol{\mu} = = \Delta\mathbf{Q} \quad (14)$$

As typical of *elastic-plastic problems*, the solution in terms of incremental quantities can be found at each time-step by exploiting a simple iterative procedure. First, for a given $\Delta\mathbf{Q}$, a vector $\Delta\mathbf{U}$=$\Delta\mathbf{U}_1$ is found by setting $\Delta\boldsymbol{\lambda}$=$\Delta\boldsymbol{\mu}$=$\mathbf{0}$. Next, the vectors $\Delta\boldsymbol{\lambda}$=$\Delta\boldsymbol{\lambda}_1$ and $\Delta\boldsymbol{\mu}$=$\Delta\boldsymbol{\mu}_1$ are determined, which would satisfy the constitutive law at the selected *strain points* if the real incremental displacements were $\Delta\mathbf{U}_1$. This allows one to compute an updated vector $\Delta\mathbf{U}$=$\Delta\mathbf{U}_2$, which satisfies (14) for $\Delta\boldsymbol{\lambda}$=$\Delta\boldsymbol{\lambda}_1$ and $\Delta\boldsymbol{\mu}$=$\Delta\boldsymbol{\mu}_1$. The process shall continue until convenient measures of the differences $\{\Delta\boldsymbol{\lambda}_i$–$\Delta\boldsymbol{\lambda}_{i-1}\}$ and $\{\Delta\boldsymbol{\mu}_i$–$\Delta\boldsymbol{\mu}_{i-1}\}$ are below a given threshold.

Of course, the finite element formulation discussed above does have practical relevance, if the parameters concerned with the material model can be estimated with reasonable accuracy and confidence.

This issue is the object of the next Section. Here, numerical simulations of experimental tests will be considered and it will be shown that the required parameters can be effectively determined (at the very least) by means of quasi-static compression tests.

III. Estimate of the Parameters Needed for the *Generalized Voigt Model*

In order to estimate the parameters required for the numerical *viscoelastic-plastic analysis* discussed in the paper, traditional optimization techniques can be considered. For instance, we performed some preliminary tests by using the *Kalman filtering technique* [6], which was already adopted in the past to estimate parameters concerned with time-dependent problems [7, 8].

However, despite initial satisfactory results, we eventually preferred to focus on a simple *trial and error* approach, even though it is usually not particularly efficient under a computational point of view, since it tends to be time-consuming. Nonetheless, it seems quite interesting and valuable, since it is suitable to exploit typical features of the *generalized Voigt model* that represents the object of the present work.

The first thing that was clear was that, unfortunately, the elastic constants, responsible for the instantaneous response of the material to external actions, could hardly be estimated in a direct way because of the dominant effects due to the viscous behavior (no matter what algorithm is selected to determine optimal values of the unknown parameters).

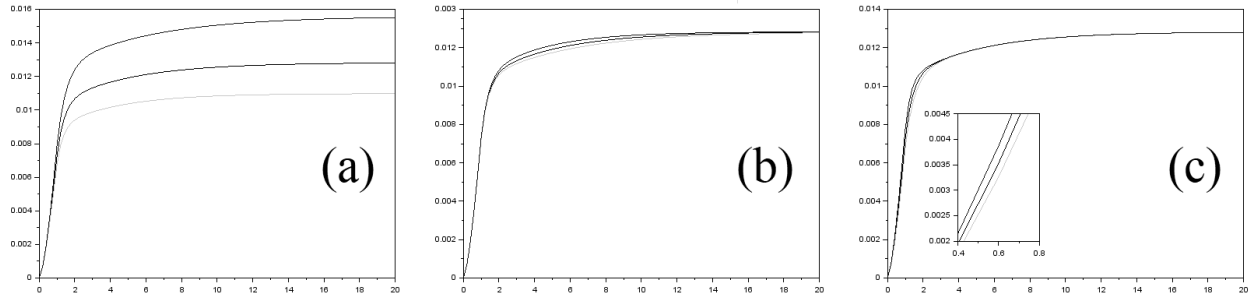

Fig. 4. *Effect of the parameters of E^*, η_V, and η_D on the viscoelastic response of a cylindrical specimen subjected to a compression test (units: mm, s).*

However, it was also possible to notice some peculiarities, which proved to be very useful for the estimate of the parameters concerned with the *viscoelastic, time-dependent response*, which was the object of some initial simulations. In fact, we started with a *simplified problem* (without including non-reversible, plastic strains) in order to focus on the *viscous behavior* of the material and check the feasibility of a procedure, which was only aimed at estimating the parameters concerned with the

viscoelastic response. Obviously, the final goal was the development of an algorithm that would be able to take advantage of the main features of the material and guarantee the convergence to the optimal solution with a good degree of reliability.

As we focused on the *viscoelastic response* of specimens subjected to compression loads, we noticed that the plots of Figure 4 could be quite instructive, since they clearly showed the effect of different values of the elastic modulus E^* (4a), coefficient η_V (4b) and coefficient η_D (4c) of the *generalized Voigt model* when plastic strains are ruled out. It was possible to observe that the largest value of the displacement is hardly affected by η_V and η_D, while it dramatically depends on Young's modulus E^* concerned with the time-dependent response. As suggested by (2), E^* denotes the elastic stiffness parameter concerned with the *generalized Voigt model* and related to the stiffness parameters K^* and G^* in (3). Of course, it has nothing to do with the elastic modulus E of the material (related to K and G in the same equations), responsible for the instantaneous, instantaneously reversible response in terms of strains induced by given stresses.

More precisely, the curves in the middle in the plots of Fig. 4 refer to the vertical deformation computed for a cylindrical specimen (with radius r=50 mm and thickness w=70 mm) subjected to uniaxial compression, assuming E=2000 MPa, E^*=320 Mpa, η_V=2000 MPa s, η_D=50 MPa s. As for Poisson's ratio, we set it equal to 0.35 when we had to determine both the instantaneous response and the viscoelastic response. In other words, the bulk moduli (K and K^*) and the shear moduli (G and G^*) in (3) were computed by assuming the same value for Poisson's ratio, while the elastic moduli were E and E^*, respectively.

The finite element method was applied by using the mesh in Figure 2b. As for the loading condition, we imposed a uniform, maximum pressure of 0.5 N mm^{-2} applied to the upper face, linearly increasing during a time interval of 1 s and maintained constant for 19 s. The load history was subdivided into 100 time steps of 0.2 s. In addition, the following displacements of the discrete model (*cf.* Figure 2b) were constrained: normal displacements along the planes x=0, y=0 and z=0, as well as in-plane displacements of the upper face (external surface orthogonal to the z-axis), which was subjected to the external load.

The inner curves in Figure 4 show how the response is affected by a 20% increment of E^*, η_V and η_D, while the outer plots are referred to a 20% decrement of the same parameters. Besides the obvious role played by the elastic modulus E^* (Fig. 4a), the most interesting (and practically useful) consequence of lower or higher values of the parameters is the influence of η_D on the initial slope of the curves, as shown by the detailed picture in Fig. 4c. Instead, η_V appears to have some effects on the curvature of the plot in the zone where the viscous strains begin to change the shape of the graphs and nearly horizontal branches start to develop.

Therefore, in view of the above properties, it seemed reasonable to estimate the three parameters by considering a given set of *fictitious* measured displacements $\tilde{\mathbf{u}}$ and implementing a convenient *trial and error* process. Needless to say, measurements are *fictitious* since all the numerical results presented in this paper are referred to simulated tests.

As already observed, in principle the elastic properties of the material E and v, as well as Poisson's ratio v^*, should also be considered to define the *generalized Voigt model* in a detailed way. However, we eventually came to the conclusion that a good compromise could be reached by setting v=v^*=0.35 (which is a kind of usual Poisson's ratio for bituminous mixture), by assuming different values of E and by determining the best estimates of the unknown parameters E^*, η_V and η_D for each value of E. After that, it is possible to introduce a convenient *error indicator* (say λ) and find out which value of E corresponds to the least value of λ. For instance, the *error indicator* can be defined as the square root of $(\{\mathbf{u}_C-\tilde{\mathbf{u}}\}^{\mathrm{T}}\ \{\mathbf{u}_C-\tilde{\mathbf{u}}\}/\{\tilde{\mathbf{u}}^{\mathrm{T}}\ \tilde{\mathbf{u}}\})$, if the vector $\mathbf{u}_C$ denotes computed displacements (in this case the displacements determined by using v=v^*=0.35, an arbitrary value of E and the parameters E^*, η_V and η_D estimated for any selected value of E).

Clearly, the procedure can be enhanced by estimating E^*, η_V and η_D for different values of v and v^* as well, but we always assumed v=v^*=0.35 for the sample problems discussed here.

In view of the above comments, we started with an iterative scheme (*i.e.*, a possible *trial and error* process which was aimed at estimating E^*, η_V and η_D after assuming arbitrary, realistic values of E, v and v^*). Its main steps can be summarized as follows:

1. Set i=1 in order to identify the first iteration
2. On the basis of arbitrary initial values of η_V and η_D (which have limited influence on the largest displacement), find an optimal estimate of E^* by increasing or decreasing this parameter (with progressively decreasing increments or decrements) until a convenient measure of the difference between the last computed and measured displacement is below a given tolerance (say χ_E)
3. On the basis of an arbitrary initial value of η_V (which has limited influence on the initial slope of the curve) and by using the estimated parameter E^*, find an optimal value of η_D by increasing or decreasing this parameter (with progressively decreasing increments or decrements) until a convenient measure of the difference between the computed and the given slope is below a given tolerance (say χ_D)

4. On the basis of the previous estimates of E^* and η_D, find an optimal value $(\eta_V)_i$, where i denotes the current iteration, by increasing or decreasing this parameter (with progressively decreasing increments or decrements) with the aim of reducing the *error indicator* λ, until a convenient measure of the difference between the last two values of η_V is below a given tolerance (say χ_V)
5. On the basis of the previous estimates of the other parameters, find an optimal value of E^* by using the same tolerance χ_E and the same criterion adopted above (point 2)
6. On the basis of the previous estimates of the other parameters, find an optimal value of η_D by using the same tolerance χ_D and the same criterion adopted above (point 3)
7. Set $i=i+1$ and go back to point 4 until a convenient measure of the difference $(\eta_V)_i-(\eta_V)_{i-1}$ is below a given threshold (say ψ_V)

Note that the steps 4-7 must be repeated a few

times, because the impact of η_V and η_D on the largest displacement and/or the initial slope cannot be completely ignored, even though their influence is actually "limited". Similarly, E^* and η_D somehow do affect the initial slope, while the *error indicator* λ obviously depends on every parameter.

This procedure appears to be quite effective, since it tends to provide reasonable estimates, but poor accuracy is inevitable in the presence of measuring/modelling errors. Indeed, in the ideal case of a numerical simulation (without measuring/modelling errors) in which we also assume the correct values of E, v and v^*, the search for a parameter E^* which tends to give the correct final displacement and a parameter η_D which tends to give the correct initial slope of the displacement *vs.* time plot can only minimize the *error indicator* λ. Instead, when the selected parameters E, v and v^* are not correct and/or measuring/modelling errors come into play (as inevitable in real cases) the proposed approach can still provide fairly good estimates, but a parameter E^* that optimizes the final displacement and/or a parameter η_D that optimizes a certain slope do not necessarily lead to the minimum value of the *error indicator*, which takes into account the overall response of the specimen and (in this context) represents the most critical item.

Therefore, it is definitely necessary to consider a second and last phase of the estimation process, in order to correct the previous estimates of the parameters by adopting a strategy, which aims at minimizing the *error indicator* λ at each step, whenever a parameter is updated (not only when we deal with η_V, but also when positive or negative increments are imposed to E^* and η_D).

Again we decided to proceed through an iterative scheme by increasing or decreasing the unknown parameters with progressively decreasing increments or decrements. At the first iteration (or, alternatively, at the *j-th* iteration with $j=1$), we updated the parameters estimated at the end of the previous phase (first E^*, next η_V, finally η_D) until the absolute values of the relevant increments or decrements were within a given tolerance (say χ). At the end of the first iteration, the *error indicator* (say λ_1) was obviously less than its value at the end of the first phase.

Then, we computed new values of λ (say λ_j, with $j=2, 3, \ldots$) by using the same *trial and error* algorithm, by estimating (in turn) E^*, η_V and η_D and by assuming (each time, as initial values) the last estimates of the *a priori* unknown parameters. The process continued until a convenient measure of the difference $\Delta\lambda=\lambda_j-\lambda_{j-1}$ was less than a given tolerance (say ψ_λ).

In order to check whether the proposed methodology succeeded in providing reliable estimates, we carried out some numerical simulations by generating a set of displacements (assumed as *fictitious* measured data) and tried to find optimal values of E^*, η_V and η_D.

The *fictitious* measurements (vertical deformations) were determined by considering the same mechanical properties, the same mesh, the same loading condition and the same time steps that provided the curve in the middle of each plot in Fig. 4. Next, for the estimate of the parameters, we used exactly the same discrete model and same compression load, ruling out modelling errors. Consequently, a correct estimate of the parameters was expected, provided that sufficiently tight tolerances had been selected.

The *trial and error* algorithm was applied by assuming a set of different values for E (including the correct value $E=2000$ MPa) and by using, for any given elastic modulus, the following initial values of the parameters, which were assumed to be *a priori* unknown: $E^*=100$ MPa, $\eta_V=1$ MPa s and $\eta_D=1$ MPa s for the estimate of E^*, again $\eta_V=1$ MPa s and $\eta_D=1$ MPa s for the estimate of η_D and $\eta_D=1$ MPa s for the estimate of η_D. In addition, adequate termination criteria were needed:

- During the first phase, each estimation process aimed at finding an optimal value of the parameter E^* was stopped when $|(u_L-\hat{u}_L)/\hat{u}_L|<\chi_E=0.01$, where u_L and $\hat{u}_L$ are the last computed and measured displacement, while $|[*]|$ denotes the absolute value of the quantity $[*]$; similarly, the estimation process to find an optimal value of the parameter η_D was stopped when $|(s-\hat{s})/\hat{s}|<\chi_D=0.01$, where $s=\Delta u/\Delta T$ and $\hat{s}=\Delta\hat{u}/\Delta T$, if Δu and $\Delta\hat{u}$ denote the differences between the increments of the computed and measured displacements during a time interval concerned with the initial portion of the curve (*e.g.*, for the sample problem discussed here, we set $\Delta T=t_2-t_1$ with $t_1=0.6$ s and $t_2=1$ s)

- As for η_V, again during the first phase, each estimation process was stopped when a parameter $(\eta_V)_i$ was obtained, such that $\Delta\eta_V/\eta_V^* < \chi_V = 0.001$, where $\Delta\eta_V$ denotes the absolute value of the last increment of η_V and η_V^* its penultimate estimate during the *i-th* iteration; hence, $\Delta\eta_V = |(\eta_V)_i - \eta_V^*|$
- During each iteration of the second phase, every parameter was updated until the absolute value of its last increment divided by the penultimate estimate was below the threshold $\chi = 0.0001$
- The following conditions had to be satisfied in order to complete the two phases: $|(\eta_V)_i - (\eta_V)_{i-1}|/(\eta_V)_{i-1} < \psi_V$, with $\psi_V = 0.01$, and $|\lambda_j - \lambda_{j-1}|/\lambda_{j-1} < \psi_\lambda$, with $\psi_\lambda = 0.01$

By means of the numerical simulations, it was possible to check that the algorithm does converge towards the correct solution, when Young's modulus E is assumed to be equal to 2000 MPa. As expected, the *error indicator* λ tends to increase when an elastic modulus E is assumed whose difference with respect to the true value (2000 MPa) is larger. Some significant results are reported in Table II, which also provides the percentage errors of each estimate, determined by computing the ratio $(Q - \bar{Q})/\bar{Q}$ multiplied by 100, where Q denotes a certain estimate and $\bar{Q}$ the corresponding correct parameter.

These results seem to prove that the procedure envisaged in this paper is actually able to estimate the parameters concerned with the *generalized Voigt model* (under the assumption that a *viscoelastic behavior* can be considered). However, a material model must take non-reversible strains into account in order to properly describe the behavior of *bituminous mixtures*. Thus, we introduced plastic strains with the aim of enforcing constant strain rates (at each strain point) when the load is maintained constant, as typical of the so-called *secondary zone* [9] (which essentially corresponds to the nearly rectilinear branches before the peak values in the plots of Fig.5).

TABLE II. INFLUENCE OF ESTIMATES OF E^*, η_V AND η_D FOR $\nu = \nu^* = 0.35$ AND DIFFERENT VALUES OF E, WITH PERCENTAGE ERRORS IN BRACKETS (UNITS: MPa FOR YOUNG'S MODULI, MPa s FOR THE VISCOUS PARAMETERS).

E	E^* (% error)	η_V (% error)	η_D (% error)	λ
1000	3.804592e+02 (18.8935)	2.717463e+03 (35.87315)	8.310358e+01 (66.20716)	5.522849e-03
1500	3.375412e+02 (5.481625)	2.239279e+03 (11.96395)	5.868962e+01 (17.37924)	1.639441e-03
2000	3.199581e+02 (-0.0130937)	2.003706e+03 (0.1853)	4.999979e+01 (-0.00042)	5.619753e-05
2500	3.103316e+02 (-3.021375)	1.872460e+03 (-6.377)	4.555551e+01 (-8.88898)	9.103492e-04
3000	3.040467e+02 (-4.9854063)	1.806958e+03 (-9.6521)	4.281226e+01 (-14.37548)	1.487575e-03

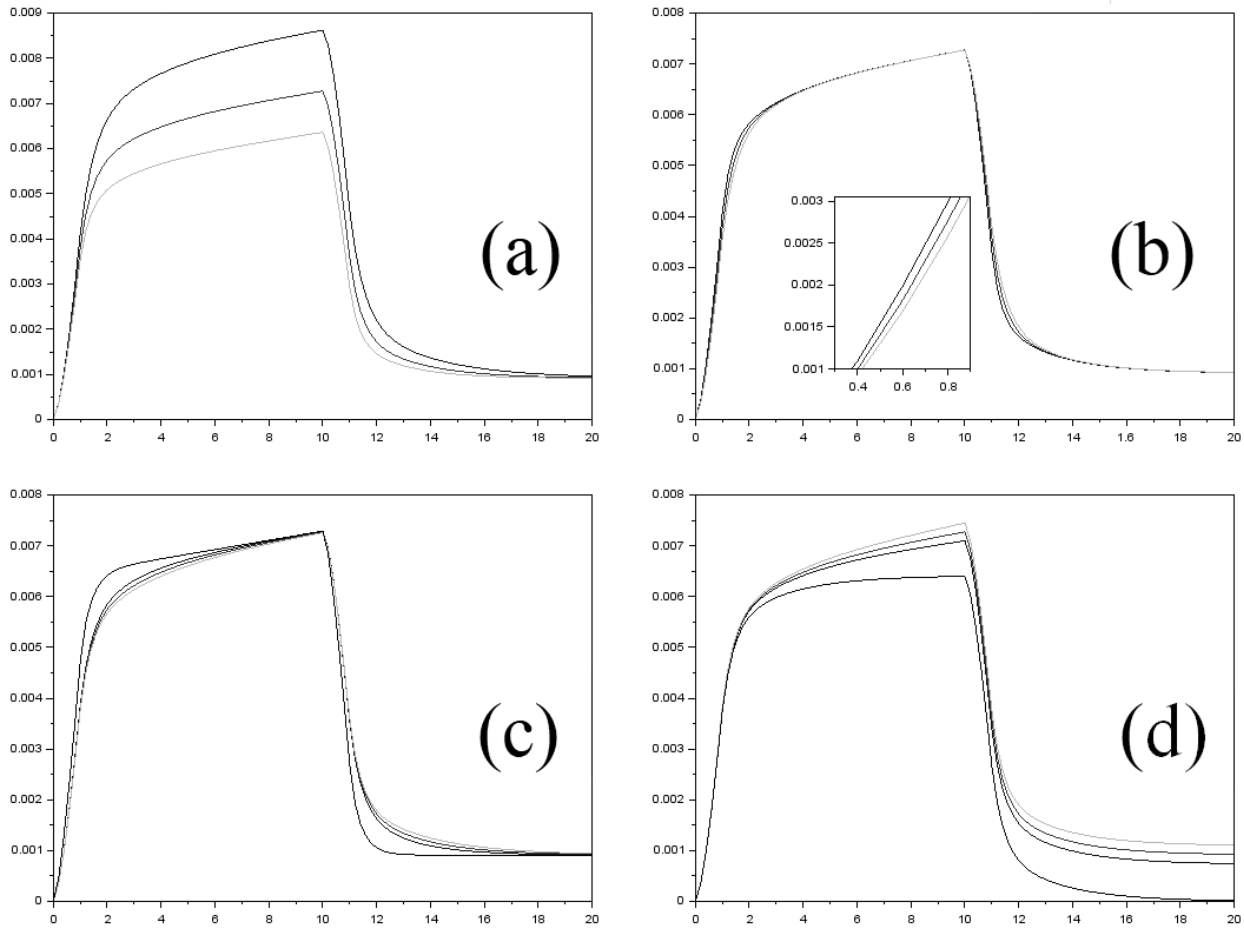

Fig. 5. *Effect of the parameters E^*, η_V, η_D and β on the viscoelastic-plastic response of a cylindrical specimen subjected to a compression test (units: mm, s).*

More precisely, for this preliminary study we simply considered plastic strain rates given by the equations $\Delta\boldsymbol{\varepsilon}^p/\Delta t=\beta\,(\boldsymbol{\varepsilon}_m-\boldsymbol{\varepsilon}^p)$ and $\Delta\mathbf{e}^p/\Delta t=\beta\,(\mathbf{e}-\mathbf{e}^p)$, where the terms in

brackets represent the current reversible volumetric and deviatoric strains, proportional to the corresponding stresses in the case of linear elasticity.

As we did before while dealing with *viscoelastic materials*, we began to check how each parameter affects a specimen subjected to a compression test. The relevant results are shown in Fig. 5.

There are clear similarities with the case of *viscoelastic materials*, since E^* does affect the largest displacements (Fig. 5 a) and η_D the initial slopes (Fig. 5 b). In fact, higher values of these parameters imply lower values of the displacements and slopes, respectively. Instead, η_V seems to have minor specific effects (*cf.* Fig. 5c, in which the curve characterized by a horizontal line on the right hand side was obtained with the extremely low value η_V=1 MPa s). As for β, it is obviously responsible for the residual displacements (*cf.* Fig. 5d, in which the curve that tends to zero was obtained by imposing an extremely low value of β, namely β=0.0001 s^{-1}).

Apart from the curves concerned with η_V=1 MPa s and β=0.0001 s^{-1}, Fig. 5 shows the displacement-time plots obtained by assuming the mechanical properties E=4000 MPa, $\nu=\nu^*$=0.35, E^*=640 MPa, η_V=2000 MPa s, η_D=100 MPa s, β=0.01 s^{-1}, together with the graphs due to a 20% increment or a 20% reduction of E^* (Fig. 5a), η_D (Fig. 5b), η_V (Fig. 5c) and β (Fig. 5d). Therefore, the three curves in Figs. 5a-b and the three contiguous curves in Figs. 5c-d were obtained by considering the mechanical properties defined above and a ±20% increment of each parameter.

In view of the specimen response and the influence of the four parameters on the displacement *vs*. time plots, we used an algorithm similar to the one implemented for the viscoelastic case. Thus, we set E^*=100 MPa, η_V=1 MPa s, η_D=1 MPa s and β=0.000001 s^{-1} for the first estimate of E^*. Such estimate was determined by imposing the condition $|(u_P-\hat{u}_P)/\hat{u}_P|<0.01$, where u_P and $\hat{u}_P$ denote the peak computed and measured displacement. Then, we estimated η_D with the aim of optimizing the initial slope of the plots: as before, the *trial and error* process was stopped when $|(s-\hat{s})/\hat{s}|$ became less 0.01. Next, the *error indicator*, given by the scalar product $(\{\mathbf{u}_C-\tilde{\mathbf{u}}\}^T\{\mathbf{u}_C-\tilde{\mathbf{u}}\}/\{\tilde{\mathbf{u}}^T\,\tilde{\mathbf{u}}\})$, was reduced by adjusting η_V until $\Delta\eta_V/\eta_V^*<0.01$. As before, $\Delta\eta_V$ denotes the absolute value of the last increment of η_V, while η_V^* is the

penultimate estimate, so that we can set $|(\eta_V)_i - \eta_V^*| = \Delta\eta_V$. Finally, a first estimate of the coefficient β was found by minimizing the difference between the last computed and measured displacement (u_L and $\hat{u}_L$, respectively). In this case, the algorithm was stopped when $|(u_L - \hat{u}_L)/\hat{u}_L| < 0.01$.

Then, we preferred to go straight to the second phase and adjust every parameter with the only objective of reducing the *error indicator*, without further attempts to improve the estimates by enforcing given values of significant displacements and/or initial slopes. Again, this second phase essentially consisted of an iterative procedure, whose purpose was to update (in turn) the parameters E^*, η_V, η_D and β. The process continued (for each parameter) until the ratio $|\Delta p/p|$ became less than 0.01, where Δp represents the last increment or decrement of the parameter to be updated, while p denotes its penultimate estimate.

A few results, quite encouraging, are reported in Table 3. They consist of a first set of estimates and were determined by assuming $\nu = \nu^* = 0.35$ and E=3000, 4000, 5000 MPa). The final (optimal) values are definitely accurate when E=4000 MPa (*i.e.*, when the correct elastic modulus was assumed), even if they were obtained by adopting a rather loose tolerance to stop the estimation process. In fact, the overall procedure was completed when $|\lambda_j - \lambda_{j-1}|/\lambda_{j-1} < \psi_\lambda = 0.1$, where λ_j denotes the *error indicator* at the end of the *j-th* iteration (*i.e.*, at the end of the *j-th* sequence of operations needed to improve the estimates of the four unknown parameters during the second phase). The estimate η_V=1 MPa s, obtained for E=5000 MPa, was due to a lower limit imposed by the algorithm.

TABLE III. ESTIMATES OF E^*, η_V, η_D AND β (PERCENTAGE ERRORS IN BRACKETS) OBTAINED WITH THREE VALUES OF E, $\nu = \nu^* = 0.35$ AND $\psi_\lambda = 0.1$ (UNITS: MPa FOR YOUNG'S MODULI, MPa s FOR THE VISCOUS PARAMETERS, s^{-1} FOR β).

E	E^* (% error)	η_V (% error)	η_D (% error)	β (% error)	λ
3000	6.855077e+02 (7.1105781)	1.822693e+03 (-8.86535)	1.210076e+02 (21.0076)	7.895153e-02 (-21.04847)	4.934916e-03
4000	6.415035e+02 (0. 2349219)	1.951153e+03 (-2.44235)	1.004670e+02 (0.467)	1.009087e-01 (0.9087)	6.479765e-04
5000	6.401686e+02 (0.0263437)	1.000000e+00 (-99.95)	1.825408e+02 (82.5408)	1.405851e-01 (40.5851)	1.563920e-02

As expected (and as confirmed by Table III), the *error indicator* attains its minimum value when Young's modulus is assumed to be equal to the correct value (4000 MPa). Thus, once more the proposed strategy appears to be able to provide reliable estimates.

The same trend can be observed if a stricter tolerance is imposed, as shown in Table IV, which is concerned with the estimates of the same parameters determined by setting ψ_λ=0.01 and ψ_λ=0.001.

Also in the case of Table IV, the final estimates of the parameter η_V (1 MPa s), obtained by assuming an elastic modulus E=5000 MPa, were enforced by the algorithm, which set a lower limit to this parameter. Instead, the same results obtained for E=4000 MPa depend on the fact that each parameter was updated (with the aim of reducing the *error indicator* λ) until the ratio $|\Delta p/p|$ defined above was less than 0.01. Had a stricter tolerance been chosen, different estimates would have been found. algorithm.

TABLE IV. ESTIMATES OF E^*, η_V, η_D AND β (PERCENTAGE ERRORS IN BRACKETS) OBTAINED WITH THREE VALUES OF E, $\nu = \nu^* = 0.35$

(UNITS: MPa FOR YOUNG'S MODULI, MPa s FOR THE VISCOUS PARAMETERS, s^{-1} FOR β).

E	E^* (% error)	η_V (% error)	η_D (% error)	β (% error)	λ (ψ_λ)
3000	6.783449e+02 (5.9913906)	2.058673e+03 (2.93365)	1.174217e+02 (17.4217)	7.609785e-02 (-23.90215)	3.100872e-03 (0.01)
4000	6.403298e+02 (0.0515312)	1.989842e+03 (-0.5079)	1.000875e+02 (0.0875)	1.001966e-01 (0.1966)	1.395015e-04 (0.01)
5000	6.400126e+02 (0.0019688)	1.000000e+00 (-99.95)	1.814044e+02 (81.4044)	1.413918e-01 (41.3918)	1.558664e-02 (0.01)
3000	6.762776e+02 (5.668375)	2.127554e+03 (6.3777)	1.166500e+02 (16.65)	7.526599e-02 (-24.73401)	2.937676e-03 (0.001)
4000	6.403298e+02 (0.0515312)	1.989842e+03 (-0.5079)	1.000875e+02 (0.0875)	1.001966e-01 (0.1966)	1.395015e-04 (0.001)
5000	6.407941e+02 (0.1240781)	1.000000e+00 (-99.95)	1.806522e+02 (80.6522)	1.419618e-01 (41.9618)	1.555619e-02 (0.001)

Of course, a real case would require several estimates of the unknown parameters by assuming (at the very least) different values of Young's moduli. However, different values of Poisson's ratios should also be considered in order to obtain more accurate results.

The obvious consequence is that the identification procedure is necessarily time-consuming. However, it is worth noting that *reasonable, initial values* of Young's moduli can be determined quite easily by means of high-frequency measures of the vertical deformation during an unloading phase. Indeed, the displacement increments which take place during a very short time interval (*e.g.*, 0.001 s) essentially depend on the linear elastic response. Thus, the ratio of the load increment per unit surface to the strain increment will provide a "reasonable" estimate of Young's modulus.

Obviously, the estimate will be approximate (and, hence, just "reasonable") because a uniform stress/strain distribution would be needed in order to find an exact value (apart from measurement errors). For instance, by performing an elastic analysis with the discrete model utilized in this work (for which we assumed E=4000 MPa and enforced zero in-plane displacements along the loaded face, in order to simulate the friction between the specimen and the loading plate), the ratio of the load increment per unit surface to the strain increment turned out to be about 3956 MPa, with an error which was slightly greater than 1%.

Finally, it can be stressed that the *generalized viscoelastic-plastic model* discussed here is also suitable to compute the displacements of a specimen subjected to a *static compressive creep test* when the load is maintained constant for a relatively long time and the so-called *tertiary deformation* occurs, which is characterized by a large increase in compliance and only implies *deviatoric strains* [9]. As a matter of fact, the material model considered in this paper is based on a clear distinction between volumetric and deviatoric effects. Therefore, the behavior of a test specimen concerned with the *tertiary zone* can be easily described by setting η_V=0 MPa s and properly calibrating the viscous coefficient η_D.

IV Closing Remarkss

A *viscoelastic-plastic material model*, which is able to deal with three-dimensional stress states and distinguishes deviatoric effects from volumetric effects, has been considered. Next, it was implemented in the framework of a 3D finite element package based on 15-node pentahedral and 20-node hexahedral elements. Thus, by means of simulated compression tests on cylindrical specimens, it was possible to show that the relevant parameters can be estimated with a satisfactory degree of accuracy.

As a matter of fact, some preliminary results are quite promising and the computer package developed so far appears to be suitable to proceed with a further phase of this study, which shall certainly consist of the estimate of parameters concerned with real specimens. Of course, the same procedure shall be applied and, hence, the experimental data shall be concerned with compression tests characterized by single loading/unloading cycles, in full analogy with the simulated tests, which have been the main object of this paper.

Next, at the very least, it will be necessary to consider specimens made of the same material, apply some significant load conditions (*e.g.*, indirect tension, pulse loads, sine loads) and compare the experimental measurements with the numerical results. In this way, it will be possible to check whether the *viscoelastic-plastic material model* presented here does succeed in describing the actual behavior of *bituminous mixtures* in the presence of different external forces. Clearly, this is an essential requirement to establish that the *generalized Voigt model* is really adequate for the analysis and design of pavements.

References

[1] J. Neves, A. Gomes-Correia, "Evaluation of the stiffness modulus of bituminous mixtures using laboratory tests (NAT) validate by field back-analysis", in Proceedings Seventh International Conference on the Bearing Capacity of Roads, Railways and Airfields (edited by I. Horvli), 7th BCRRA Conference, Trondheim, Norway 25 - 27 June 2005.

[2] M.R. Taha, S. Hardwiyono, N.I.Md. Yusoff, M.R. Hainin, J. Wu, K.A.M. Nayan, "Study of the Effect of Temperature Changes on the Elastic Modulus of Flexible Pavement Layers", Research Journal of Applied Sciences, Engineering and Technology, 5(5), 1661-1667, 2013.

[3] A. Setiawan, L.B. Suparma, A.T. Mulyono, "Developing the Elastic Modulus Measurement of Asphalt Concrete Using the Compressive Strength Test", in AIP Conference Proceedings 1855, 2017.

[4] European Committee for Standardization, "Bituminous mixtures - Test methods for hot mix asphalt – Part 26: Stiffness", Final Draft prEN 12697-26, December 2003.

[5] A. Schmidt, L. Gaul, "FE Implementation of Viscoelastic Constitutive Stress-Strain Relations Involving Fractional Time Derivatives", Nonlinear Dynamics, 29-37, 2002.

[6] P. Eikhoff, "System Identification", John Wiley, Chichester, 1983.

[7] S. Bittanti, G. Maier, A. Nappi, A., "Inverse problems in structural elastoplasticity: a Kalman filter approach", in Plasticity today: modelling, methods and applications (eds.: by A. Sawczuk and G. Bianchi), Elsevier A.S.P., Amsterdam, 311-329, 1984.

[8] A. Nappi, S. Rajgelj, "Estimate of damage effects in large dams: A Kalman filtering approach", in

Advances in Computational Engineering and Sciences (edited by S.N. Atluri and D.W. Pepper), Tech Science Press, Encino, California, 2002.

[9] M.W. Witczak, K. Kaloush, T. Pellinen, M. El-Basyouny, H. Von Quintus, NCHRP Report 465, National Academy Press, Washington, D.C., 2002.